AGU PUBLICATIONS

JGR

Journal of Geophysical Research: Atmospheres

RESEARCH ARTICLE
10.1002/2014JD021936

Key Points:
- Western China has higher surface O_3 concentrations compared with Eastern China
- Foreign Eurasian emissions contribute 10–15 ppbv surface O_3 over Western China
- Mitigation of emissions from EU and IN could benefit public health in Western China

Supporting Information:
- Readme
- Figures S1–S6

Correspondence to:
J. Liu,
jfliu@pku.edu.cn

Citation:
Li, X., J. Liu, D. L. Mauzerall, L. K. Emmons, S. Walters, L. W. Horowitz, and S. Tao (2014), Effects of trans-Eurasian transport of air pollutants on surface ozone concentrations over Western China, *J. Geophys. Res. Atmos.*, *119*, 12,338–12,354, doi:10.1002/2014JD021936.

Received 24 APR 2014
Accepted 30 SEP 2014
Accepted article online 3 OCT 2014
Published online 6 NOV 2014

Effects of trans-Eurasian transport of air pollutants on surface ozone concentrations over Western China

Xiaoyuan Li[1,2,3], Junfeng Liu[1], Denise L. Mauzerall[4,5], Louisa K. Emmons[6], Stacy Walters[6], Larry W. Horowitz[7], and Shu Tao[1]

[1]Laboratory for Earth Surface Processes, College of Urban and Environmental Sciences, Peking University, Beijing, China, [2]College of Physics, Peking University, Beijing, China, [3]Now at Department of Civil and Environmental Engineering, Princeton University, Princeton, New Jersey, USA, [4]Woodrow Wilson School of Public and International Affairs, Princeton University, Princeton, New Jersey, USA, [5]Department of Civil and Environmental Engineering, Princeton University, Princeton, New Jersey, USA, [6]National Center for Atmospheric Research, Boulder, Colorado, USA, [7]NOAA Geophysical Fluid Dynamics Laboratory, Princeton, New Jersey, USA

Abstract Due to a lack of industrialization in Western China, surface air there was, until recently, believed to be relatively unpolluted. However, recent measurements and modeling studies have found high levels of ozone (O_3) there. Based on the state-of-the-science global chemical transport model MOZART-4, we identify the origin, pathway, and mechanism of trans-Eurasian transport of air pollutants to Western China in 2000. MOZART-4 generally simulates well the observed surface O_3 over inland areas of China. Simulations find surface ozone concentrations over Western China on average to be about 10 ppbv higher than Eastern China. Using sensitivity studies, we find that anthropogenic emissions from all Eurasian regions except China contribute 10–15 ppbv surface O_3 over Western China, superimposed upon a 35–40 ppbv natural background. Transport from European anthropogenic sources to Northwestern China results in 2–6 ppbv O_3 enhancements in spring and summer. Indian anthropogenic sources strongly influence O_3 over the Tibetan Plateau during the summer monsoon. Transport of O_3 originating from emissions in the Middle East occasionally reach Western China and increase surface ozone there by about 1–4 ppbv. These influences are of similar magnitude as trans-Pacific and transatlantic transport of O_3 and its precursors, indicating the significance of trans-Eurasian ozone transport in hemispheric transport of air pollution. Our study further indicates that mitigation of anthropogenic emissions from Europe, the Indian subcontinent, and the Middle East could benefit public health and agricultural productivity in Western China.

1. Introduction

Due to lack of industrialization, until recently Western China (WC) was considered relatively little affected by air pollution. However, measurements in WC have shown that surface O_3 levels are high and frequently exceed 50 ppbv during the summer [*Ran et al.*, 2014; *Xue et al.*, 2011; *Yang et al.*, 2014]. The World Health Organization (WHO) guideline for daily maximum 8 h O_3 concentration is 50 ppbv [*World Health Organization*, 2006]. High surface O_3 concentrations that exceed the WHO standard have been found to increase human mortality [*Gryparis et al.*, 2004]. WC, although less populated than Eastern China (EC), has a large population of more than 60 million [*China Statistical Yearbook*, 2013] whose health are potentially affected by O_3. High surface O_3 can also reduce agricultural production [*Avnery et al.*, 2011; *Mauzerall and Wang*, 2001; *Shindell et al.*, 2012; *Wang and Mauzerall*, 2004; *West et al.*, 2006], which was over 30×10^6 t in WC in 2013 [*China Statistical Yearbook*, 2013], and is still growing. New Chinese ambient air quality standards (to be implemented in 2016 for the whole China) set 8 h O_3 concentrations at 50 ppbv (Guobiao (GB) 3095–2012) for Grade I (i.e., Natural Protection Area and other areas which need special protection). As WC is known for large nature reserve areas, controlling surface O_3 should be important in regard to the national standards. Thus, mitigating O_3 and its precursors has a tribenefit of improving human health, food security, and environmental protection [*Mauzerall and Wang*, 2001; *Shindell et al.*, 2012; *West et al.*, 2006]. An important prerequisite to understand the potential to meet these new standards is to determine the fraction of the O_3 in WC originating from emissions within China versus the O_3 and its precursors that are advected into China from upwind regions.

Tropospheric ozone is a secondary pollutant, formed from the reactions of nitrogen oxides ($NO_x = NO + NO_2$), carbon monoxide (CO), methane (CH_4), and non-methane organic hydrocarbons ($NMOC_s$) in the presence

of sunlight. O_3 concentrations are determined by both local emissions and the long-range transport of O_3 and its precursors. Transported from the boundary layer to the free troposphere, the lifetime of O_3 and its precursors is significantly lengthened and they can travel long distances in the midlatitude westerlies. This leads to three areas of long-range transport research in the Northern Hemisphere: transatlantic, trans-Pacific, and trans-Eurasian transport [*Emmons et al*., 2010; *Wang et al*., 2009; *West et al*., 2009].

Transatlantic transport of O_3 and its precursors has been characterized with measurement and modeling studies [*Honrath et al*., 2004; *Huntrieser et al*., 2005; *Martin et al*., 2006; *Stohl et al*., 2003; *Trickl et al*., 2003]. Measurements indicated that emissions from North America take about 6 to 15 days to reach the Mid-Atlantic due to frequent transport from middle and high latitudes [*Honrath et al*., 2004; *Martin et al*., 2006; *Martin*, 2008; *Owen et al*., 2006]. Studies on trans-Pacific transport of air pollution originating in East Asia (Hemispheric Transport of Air Pollution (HTAP)) estimated an increase of monthly mean O_3 concentrations by 2–6 ppbv in the western United States and by 1–3 ppbv in the eastern United States from 1985 to 2010 [*Brown-Steiner and Hess*, 2011; *Jacob et al*., 1999]. Average trans-Pacific transport time is usually in the range of 2–3 weeks in April [*Liu et al*., 2005; *Liu and Mauzerall*, 2005]. However, under certain conditions, Asian emissions can be transported rapidly across the Pacific in the form of strong episodes that contribute 8–15 ppbv ozone on days when observed daily maximum 8 h average ozone exceeds 60 ppbv [*Brown-Steiner and Hess*, 2011; *Lin et al*., 2012].

Trans-European transport, leading to European air pollution adversely impacting air quality in Asia, has been documented from ground-based observations at Mondy in eastern Siberia [*Pochanart et al*., 2003], together with modeling suggestions above the Middle East (ME) and Mediterranean Sea [*Li et al*., 2001]. Simulated trans-Eurasian transport of O_3 and its precursors led to monthly mean O_3 enhancements over Siberia of about 0.5–3.5 ppbv and a smaller influence over Japan of about 0.2–2.5 ppbv around the year1996 [*Wild et al*., 2004]. The Middle East is an area that is frequently examined in trans-Eurasian related research because it is affected by both Asian and European outflows (primarily through Mediterranean Sea) [*Liu et al*., 2009], due to the anticyclonic circulation in the middle and upper troposphere above the ME [*Li et al*., 2001]. Ozone transported from Asia to the ME exceeded that locally produced accounting for 31% and 23%, respectively [*Liu et al*., 2011]. Transport from the boundary layer over the Mediterranean Sea to the midlatitudes of the ME accounted for about 6% of its total source [*Liu et al*., 2009].

Recently, a number of studies have investigated Eastern China's surface O_3 concentrations [*Yang et al*., 2011], mainly because Eastern China (EC) is one of three regions in the world with the highest summertime surface O_3 concentrations (the other two being southeastern North America and Europe) [*David and Nair*, 2011; *Jain et al*., 2005; *Marrero et al*., 2011; *Naja et al*., 2003; *Wang et al*., 2008; *Yang et al*., 2011]. Hong Kong, Guangzhou, Shanghai, and Beijing lie in the three main industrial and most developed regions in China. Observations have focused over these regions to characterize the seasonal pattern [*Yang et al*., 2011], mechanism of chemical production [*Jain et al*., 2005], and formation of high-concentration pollution plumes [*Wang et al*., 2008]. Both observational and modeling studies consistently showed a maximum in surface O_3 concentration over Northeast China in June [*Tang et al*., 2012; *Wang et al*., 2011; *Zhao et al*., 2009]. *Tang et al*. [2012] associated it with high photochemical production and low O_3 loss due to decreased cloud cover and less dry deposition, respectively. The maximum is usually followed by a large decrease in July and August [*Li et al*., 2007; *Wang et al*., 2011], which is likely caused by the effect of summer monsoon (i.e., more clean maritime winds lead to greater ventilation) [*Wang et al*., 2011], as well as by increases in precipitation and cloud cover [*Tang et al*., 2012]. However, in WC, a summer maximum in O_3 over Waliguan, a mountainous site on the edge of the Tibetan Plateau, appears and could be explained by transport from other regions including Europe [*Pochanart et al*., 2001]. In addition, the summertime surface O_3 maximum at Waliguan was found to be influenced by stratospheric intrusions [*Ding and Wang*, 2006; *Ma et al*., 2005]. A recent study by *Wang et al*. [2013] showed distinct effects of climate change on surface O_3 concentrations and sensitivity to emissions over East China versus West China.

While most of these studies focus on EC, as it has a dense population and a higher level of economic development [*Li et al*., 2007; *Wang et al*., 2011], limited analysis has been devoted to WC. Although local emissions are small compared with EC, its location in the midlatitude westerlies suggests that surface O_3 concentrations over WC is likely to be affected by transport from the upwind regions [*Zhu et al*., 2004].

We present here a modeling investigation of the effect of trans-Eurasian air pollutants on surface O_3 concentrations over China. We evaluate the magnitude of China's background ozone in terms of seasonality and spatial distributions and establish source-receptor relationships with various source regions (domestic and foreign) and types (anthropogenic and natural) on various parts of China but with special emphasis on WC. Here we will attempt to identify the origins and transport pathways of O_3 and its precursors. The next section describes the chemical transport model and methods used in this study. In section 3, we evaluate model results and compare them with in situ observational data over China and neighboring regions. General features of China's background ozone will be shown in section 4 in terms of source types, seasonality, and regional distributions. In section 5, we identify the magnitude of influences of source regions on China's surface O_3. Section 6 describes the mechanism of trans-Eurasian ozone transport based on analyses of O_3 flux, chemical production rates, and episodic influence. Uncertainties associated with this study are discussed in section 7. Section 8 includes conclusions and policy-related questions.

2. Methodology

2.1. Model Description

MOZART-4 (Model for Ozone and Related chemical Tracers, version 4) is used to simulate global O_3 distributions and the associated intercontinental source-receptor relationships. MOZART-4 is a global chemical transport model for the troposphere, and its chemical mechanism includes 85 gas-phase species, 12 bulk aerosol compounds, 39 photolysis, and 157 gas-phase reactions [*Emmons et al*., 2010]. Online dry deposition is calculated, together with a calculation of photolysis rates using Fast Tropospheric Ultraviolet and Visible radiation model, which includes the impact of simulated clouds and aerosols [*Tie et al*., 2003].

Standard MOZART-4 simulations are at a horizontal resolution of approximate 2.8° × 2.8°, i.e., 128 (divided zonally) × 64 (divided meridionally) grids globally, and contain 28 sigma levels in the vertical from the surface to approximately 2.7 hPa driven by meteorology from the National Center for Atmospheric Research (NCAR) reanalysis of the National Centers for Environmental Prediction (NCEP) forecasts [*Emmons et al*., 2010; *Fishman*, 1991; *Rodgers et al*., 1991], updated every 6 h. Details about physical processes, chemical reactions, and updates over MOZART-2 were described in *Emmons et al*. [2010]. MOZART-4 uses synthetic ozone (SYNOZ) to constrain the stratospheric flux of ozone independently of the meteorological data set used [*McLinden et al*., 2000]. SYNOZ is advected as a passive tracer into the stratosphere with a specified source region (30°S–3°0N, 10–70 hPa) and production rate (400–500 Tg/yr). This method corrects the excessive annual stratospheric to tropospheric O_3 flux when using assimilated wind data and stratospheric O_3 field and makes the flux comparable to observations. However, it does not entirely eliminate the biases because the strength of the flux might be wrong in terms of seasonality and locations. *Emmons et al*. [2010] did an exhaustive evaluation on the 2000–2007 model simulation and found that it did not fully capture the spring-to-summer increase in ozone in the Northern Hemisphere midlatitudes. They attributed the underestimation to the constraint from the use of SYNOZ, as well as the low vertical resolution of the model. Except that, the model generally reproduces the seasonality of ozone concentrations globally. Since our study mainly focuses on effects of anthropogenic emissions on O_3, the biases, either due to SYNOZ or model resolution, could be perceived as a bias of the natural O_3 background. Thus, the validity of our analyses and results may not be affected.

2.2. Model Configuration

Simulations in this study used NCEP/NCAR reanalysis meteorological fields from 1999 to 2000, as dynamic input data. Emission inventories used in this study are provided with the standard version of MOZART-4. The majority of the anthropogenic emissions used here are from the Precursors of Ozone and their Effects in the Troposphere database for 2000 [*Granier et al*., 2005; *Olivier et al*., 2003], which includes anthropogenic emissions (from fossil fuel and biofuel combustion) based on the EDGAR-3 inventory [*Olivier and Berdowski*, 2001]. Fossil fuel and biofuel combustion emissions of black and organic carbon are from *Bond et al*. [2004] for 1996. For SO_2 and NH_3, anthropogenic emissions are from the EDGAR-FT2000 and EDGAR-2 databases, respectively. For Asia, these inventories have been replaced by the Regional Emission inventory for Asia with the corresponding annual inventory for each year [*Ohara et al*., 2007]. Aircraft emissions of NO, CO, and SO_2 from scheduled, charter, general aviation, and military traffic for 1999 are also included [*Baughcum et al*., 1998, 1996; *Mortlock and Alstyne*, 1998; *Sutkus et al*., 2001]. Biomass burning emissions for each year are from the Global Fire Emissions Database, version 2 (GFED-v2) [*van der Werf et al*., 2006]. For species not provided in

Table 1. Base and Sensitivity Simulations

Name of Simulation	Description
BASE	Standard emission inventory used.
GLOBE	Global anthropogenic emissions are all turned off.
EA	Anthropogenic emissions from East Asia are turned off.
EU	Anthropogenic emissions from Europe are turned off.
SI	Anthropogenic emissions from Siberia are turned off.
ME	Anthropogenic emissions from the Middle East are turned off.
MA	Anthropogenic emissions from mid-Asia are turned off.
IN	Anthropogenic emissions from India are turned off.
SEA	Anthropogenic emissions from Southeast Asia are turned off.

GFED-v2, emissions are determined by scaling the GFED-v2 CO_2 emissions by species-specific emission factors [*Andreae and Merlet*, 2001] and updates [*Granier et al*., 2005]. Emissions of isoprene and monoterpenes from vegetation are calculated online based on the Model of Emissions of Gases and Aerosols in Nature (MEGAN) [*Guenther et al*., 2006]. Other natural emissions, NO from soil and lightning, ocean dimethyl sulfide and volcanic SO_2, are included as in the standard MOZART-4 configuration [*Emmons et al*., 2010]. We specify here emission totals for the model year of 2000 as 1200 Tg yr^{-1} of CO (620 Tg yr^{-1} from anthropogenic sources), 42 TgN yr^{-1} of NO_x (excluding lightning NO_x; 30 TgN yr^{-1} from anthropogenic emissions), and 540 Tg yr^{-1} of isoprene from online MEGAN.

In this work, we conducted a base simulation (represented as BASE in Table 1) first with standard emissions described above. A second simulation was conducted with zero non-methane global anthropogenic emissions (i.e., GLOBE) in order to evaluate the global natural background without human influence (here anthropogenic emissions refer to emissions resulting from fossil fuel and biofuel combustion, but open biomass burning is not included). Then, we divided global continental regions into 11 parts as shown in Figure 1 and conducted seven sensitivity simulations with zero anthropogenic emissions from each of seven regions (Europe (EU), Siberia (SI), India (IN), East Asia (EA), Southeast Asia (SA), the Middle East (ME), and Middle Asia (MA)) respectively. These simulations are conducted to identify effects of a region's total anthropogenic emissions on global ozone distribution, different to the experiments designed in the Hemispheric Transport of Air Pollution (HTAP) model intercomparison project in which 20% reduction is used. Names of simulations and their descriptions are shown in Table 1. All simulations were conducted for 24 months from 1 January 1999 to 31 December 2000 using the same meteorological field from NCEP reanalysis as stated above. The model was spun-up for the first 12 month period. Source-receptor relationships and other analyses were determined from the last 12 month period, i.e., the year 2000.

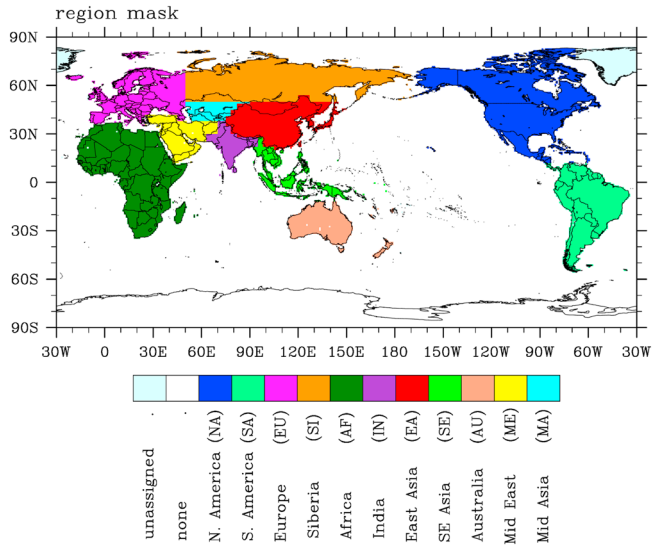

Figure 1. Eleven continental regions, in which seven regions (EU, SI, IN, EA, SE, ME, and MA) have anthropogenic emissions turned off for sensitivity simulations.

3. Model Evaluation

A global evaluation of the MOZART-4 model has been described in *Emmons et al*. [2010]. In this paper, we focus our evaluation on O_3 in order to diagnose the general performance of the model over China and neighboring regions.

3.1. Model Evaluation Over China

Measurements of O_3 at all domestic sites used in this evaluation are available in the literature. We present here comparisons with three sites:

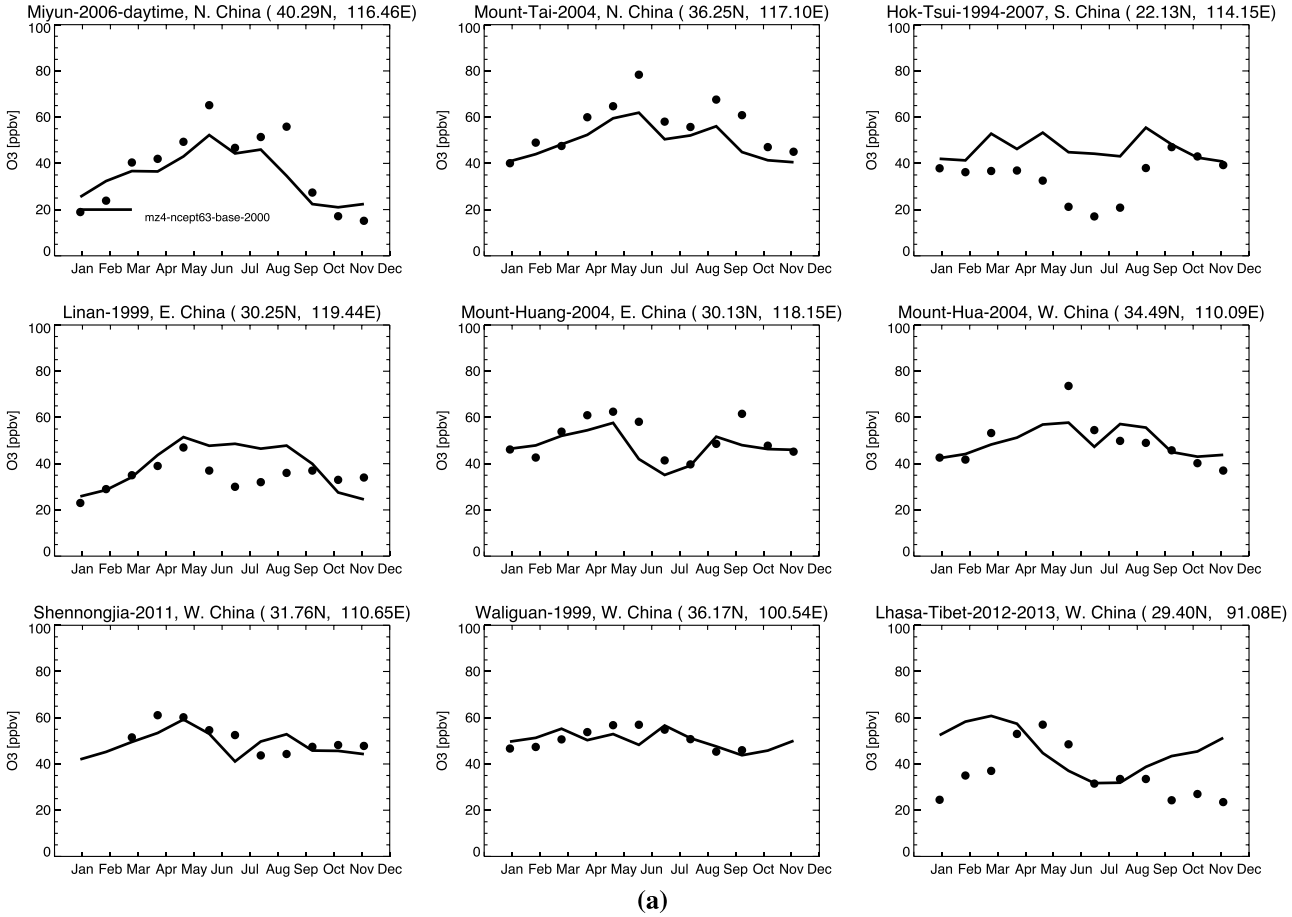

Figure 2. Simulated (lines) versus observed (dots) monthly mean concentrations (ppbv) of O_3 at surface and mountain sites over (a) China and (b) China's neighboring regions. Observational data used in each figure are the following: (first row, first column) Miyun, Northern China 2006; (first row, second column) Mount Tai, Northern China March 2004 to February 2005 (1533 m asl); (first row, third column) Hok-Tsui, Southern China average of 1994–2007; (second row, first column) Lin-An, Eastern China 1999; (second row, second column) Mount Huang, Eastern China March 2004 to February 2005 (1836 m asl); (second row, third column) Mount Hua, Western China March 2004 to February 2005 (2064 m asl); (third row, first column) Shennongjia, Western China 2001; (third row, second column) Waliguan 1999 (3810 m asl), and (third row, third column) Lhasa, Western China 2012–2013 (3650 m asl) shown in Figure 2a; (first row, first column) Mondy, Russia average of 1997–1999; (first row, second column) Inthanon, Thailand (1450 m asl); (first row, third column) Srinakarin, Thailand (Figures 2b (first row, second column) and 2b (first row, third column) are average of 1996–1998); (second row, first column) Oki, Japan (90 m asl) average of 1994–1996; (second row, second column) Ogasawara, Japan 2010; (second row, third column) Hedo, Japan 2010; (third row, first column) NPL, Mumbai, India 1998; (third row, second column) Mount Abu, India (1680 m asl) average of 1993–2000; and (third row, third column) Gadanki, India average of 1993–1996 shown in Figure 2b.

a rural site at Miyun, Beijing, (40.29°N 116,46°E, 152 m above sea level (asl)) [*Wang et al*., 2008], a rural site at Lin-An, Zhejiang Province, (30.25°N 119.44°E, 132 m asl) [*Wang et al*., 2001], and a coastal site at Hok-Tsui, Hong Kong, (22.13°N 114.15°E, 60 m asl) [*Wang et al*., 2009]. These sites are located in three of the most developed regions in China, representing surface O_3 over populated and polluted regions for years around 2000. We also compare simulated O_3 with observations at three Chinese mountain sites: Mount Tai (36.25°N, 117.10°E, 1533 m asl), Mount Hua (34.49°N, 110.09°E, 2064 m asl), and Mount Huang (30.13°N,118.15°E, 1836 m asl). Observation at these mountain sites are from *Li et al*. [2007] from March 2004 to February 2005. Furthermore, we choose three over WC: Waliguan (36.28°N, 100.90°E, 3810 m asl) for the year 2000 [*Xue et al*., 2011], which locates at the northeast edge of the Tibetan Plateau; Lhasa (29.40°N, 91.08°E, 3650 m asl) from June 2012 to May 2013 [*Ran et al*., 2014], which is the center of Tibet; and Shennongjia (31.76°N, 110.65°E) for 2001 [*Yang et al*., 2014] at the transitional zone from EC to WC.

As shown in Figure 2a, seasonal patterns of the model results match well with observations at inland (Miyun) and mountain sites (with a slight underestimation (5–10 ppbv) of O_3 concentrations during spring and summertime) but tend to overpredict O_3 near the coastal site in Hong Kong. Comparison over Hok-Tsui

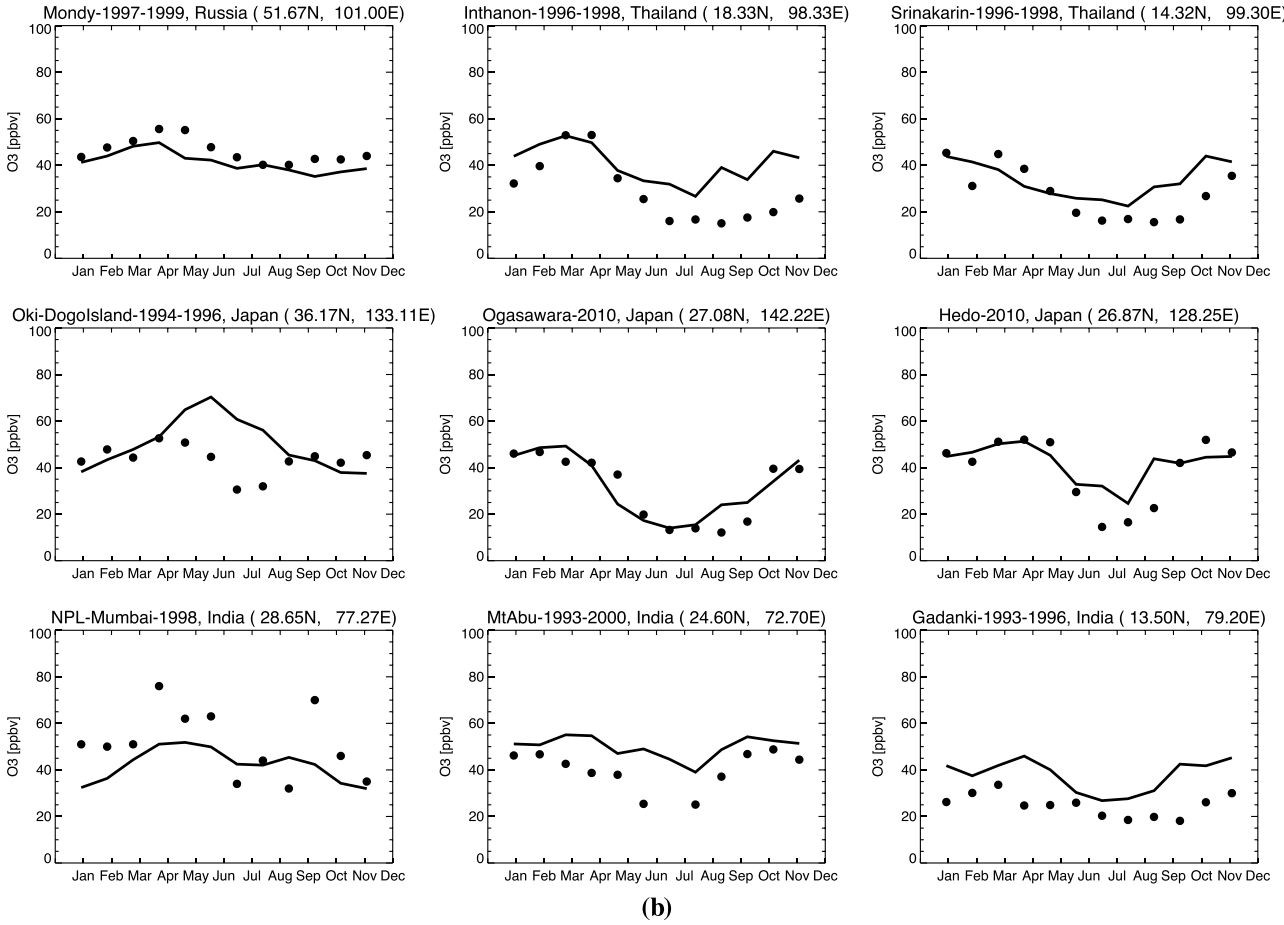

(b)

Figure 2. (continued)

presents a greater overestimate of about 10–30 ppbv in all seasons except autumn with the largest overestimates in summer. This observation site is located on the cliff at the southern edge of Hong Kong Island, dominated by sea wind and representing sea surface O_3. Wintertime results present good performance over Hok-Tsui, probably because this region is affected by inland air masses driven by East Asian monsoon in winter. Over WC, the model does not reproduce the springtime increase of surface O_3 at both Waliguan and Lhasa, which is similar to the findings by *Emmons et al.* [2010] over Northern Hemisphere midlatitudes. At Lhasa, the modeled surface O_3 agrees with the observation in spring and summer. The overestimation that occurred in autumn and winter is probably due to a titration/resolution problem, i.e., low resolution of the model causes NO_x diluted in a large grid box, which is supposed to be high near urban area like Lhasa, and the effect of O_3 titration by NO_x underestimated.

3.2. Model Evaluation Over China's Neighboring Regions

In this study, we chose nine foreign sites for comparison with observations to indicate the general performance of the model in the vicinity of China (Figure 2b). For East Asia, Mondy, Russia (51.67°N, 101.00°E, 2006 m asl) [*Li et al.*, 2007] is chosen as a site in Siberia; Oki, Japan (36.17°N, 133.11°E, 90 m asl) [*Pochanart et al.*, 1999] is chosen in Dogo Island, South Japan Sea; Hedo (26.87°N, 128.25°E) and Ogasawara (27.08°N, 142.22°E) are also chosen to provide more evaluation around Japan [*Yang et al.*, 2014]. Three sites in India are selected to evaluate O_3 in various types of locations: an urban site in Western Delhi (28.659°N, 77.279°E, 220 m asl) [*Jain et al.*, 2005], a mountain site at Mount Abu (24.6°N, 72.7°E, 1680 m asl) [*Naja et al.*, 2003], and a tropical rural site at Gadanki (13.5°N, 79.2°E, 375 m asl) [*Naja and Lal*, 2002]. For Southeast Asia, we chose two sites in Thailand: Inthanon site (18°N, 98°E, 1450 m asl) and Srinakarin site (14°N, 99°E, 296 m asl) [*Pochanart et al.*, 2001].

Comparisons show a well-matched pattern with observations in Siberia and Southeast Asia. Differences occurring at Mondy are similar to those at Miyun as described in the previous section. At Oki and Hedo, the overestimation in late spring and summer is probably because summer Asian monsoon is insufficient in extent over these regions. This weakens the cleaning effect brought by the sea wind in the model, which is quite similar to what happens in Hok-Tsui. A general overestimate in Southern India (Gadanki) is observed. This is a typical problem in most global models and is likely due to limited performance of the model on interactions between sea and land [*Hemispheric Transport of Air Pollution*, 2010]. This process cannot be simulated in the global model with low horizontal resolution, and pollutants are dispersed to neighboring areas quickly.

3.3. Summary of Model Evaluation

We have identified several biases within the model. The main problem is that the model overestimates O_3 (10−30 ppbv) in coastal areas dominated by summer monsoons. Weak interactions between land and sea in terms of air mass transport could be one of the reasons. Another major bias occurs in WC where O_3 is slightly underestimated. This bias is also indicated in a number of studies and was attributed to stratosphere-to-troposphere O_3 exchange through the use of SYNOZ, and low vertical resolution of the model [*Ding and Wang*, 2006; *Emmons et al*., 2010; *Wang and Mauzerall*, 2004]. As this study mainly focuses on anthropogenic influence, it could be perceived as a bias of the natural O_3 background.

Nevertheless, evaluations show that the model successfully represents the seasonal pattern and the magnitude of inland surface O_3 concentrations. Since this study primarily examines trans-Eurasian transport of air pollutants, model biases should not invalidate the main findings of magnitude, seasonality, and regional contributions over Eurasia, especially over WC. In the following sections, we conduct analyses for the year 2000.

4. Background Ozone Over China

Seasonal and spatial distributions of surface O_3 over China are described in this section. We also identify contributions from domestic, foreign, and natural sources. Model results from BASE, GLOBE, and EA (described in Table 1) are used to analyze China's surface ozone in terms of the natural and the anthropogenic background.

4.1. Seasonal Variability of Surface Ozone Concentrations Over China

Figure 3 shows simulated seasonal mean surface O_3 concentrations for each season over China in 2000 for the BASE simulation. Spatial patterns of China's surface O_3 indicate significant differences in seasonal variations between EC and WC. Seasonal mean O_3 concentrations for the four seasons are 20–40 ppbv (December–February (DJF)), 40–50 ppbv (March–May (MAM)), 40–50 ppbv (June–August (JJA)), and 5–35 ppbv (September–November (SON)) over EC and 40–60 ppbv (DJF), 45–55 ppbv (MAM), 35–50 ppbv (JJA), and 35–55 ppbv (SON) over WC, all in parts per billion by volume units. Year-round O_3 concentrations averaged over WC are up to 15 ppbv higher than over EC (Figure 4). Surface ozone over EC experiences a peak in spring and summer and a trough in autumn, whereas WC displays maximum in winter and minimum in summer. In EC, seasonal patterns of surface O_3 are determined by both photochemical reactions and the East Asian monsoon. In summer and spring, abundant sunlight facilitates the formation of O_3 through photochemical reactions. However, limited sunlight in winter and autumn results in NO reacting with O_3 and removing it ($NO + O_3 \rightarrow NO_2 + O_2$). While the East Asian monsoon in winter (through inflow of air with high ozone concentrations) and summer (through deposition as well as inflow of clean air from the sea) offsets this effect to some extent, EC and WC have opposite seasonal variation of surface O_3.

Seasonal variation of surface O_3 over WC, as indicated by the red line in Figure 4, especially over the Tibetan Plateau, is largely modulated by stratosphere-to-troposphere O_3 exchange [*Zhao et al*., 2010]. Our results (Figure 4) show higher surface O_3 levels in winter and spring. This could be explained by enhanced STE due o lower height of the tropopause [*Hsu et al*., 2005], although the springtime maximum found in most observations is not reproduced by the model as mentioned in section 3.3. A drop in surface O_3 over WC after spring in our simulation is observed and could be caused by weakened STE associated with high tropopause [*Zhao et al*., 2010]. However, some studies suggest that strong convection over the plateau [*Ma et al*., 2005] or horizontal transport [*Zhu et al*., 2004] may enhance surface O_3 in summer. Although summer increase is not seen in our simulation, further analysis in section 6.2 does show enhanced transport from certain source regions over WC but is offset by less transport from other sources in the Northern part and by weakened STE in the southern part.

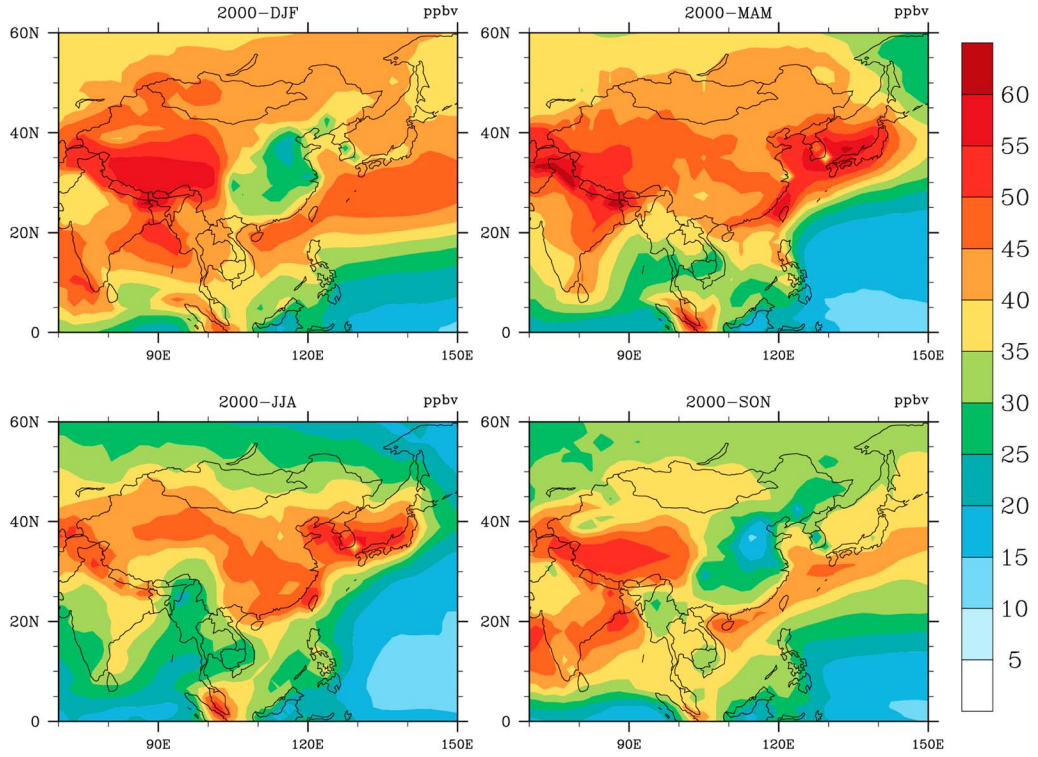

Figure 3. Spatial distributions of seasonal mean surface O_3 concentrations (ppbv) for DJF, MAM, JJA, and SON in 2000 from the BASE simulation.

4.2. China Total Background

China Total Background (CTB, described in Table 2) is defined as surface O_3 concentrations over China in the absence of anthropogenic emissions from East Asia and is simulated with all anthropogenic emissions from EA turned off. Seasonal mean CTB of 2000 is presented in Figure 5. Seasonal mean CTB over EC does not have a significant seasonal cycle and ranges from approximately 25–40 ppbv, with a slight trough in autumn of about 20–30 ppbv. The spatial pattern of CTB over EC features a minimum centered in Southeastern China, which is different from that of the BASE where minimum O_3 concentrations are centered in Northern China in autumn and winter likely due to titration of O_3 by anthropogenic NO. The difference between BASE and CTB represents the ozone enhancement caused by Chinese emissions. In EC, domestic anthropogenic emissions influence surface O_3, accounting for up to 40% of the actual concentration despite lower O_3 production efficiency resulting from higher NO_x concentrations (more will be described in section 5). CTB over WC is just a few (<5) ppbv lower than the total surface O_3 and shows the same spatial pattern. The ratio of CTB to the actual surface O_3 over WC is greater than 90%, implying that natural sources or long-range transport significantly influence WC O_3 concentrations with domestic anthropogenic emissions having limited effect on surface O_3 in WC.

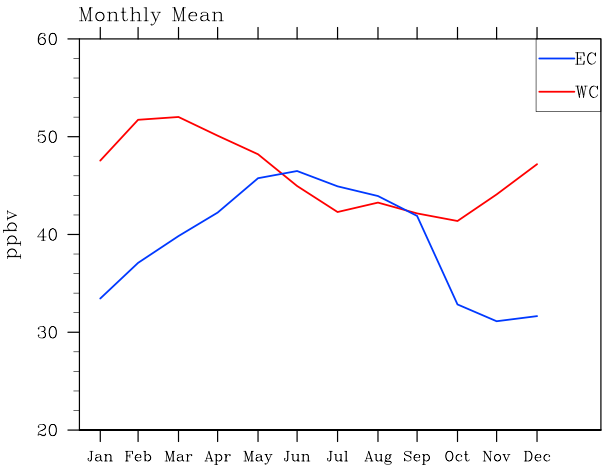

Figure 4. Monthly mean surface O_3 concentrations (ppbv) over EC (22.5°N–45°N, 100°E–120°E, indicated by the blue line) and WC (30°N–45°N, 80°E–100°E, red) in 2000 from the BASE simulation.

Table 2. Acronym Used in Analyses

Acronym	Description
CTB	China Total Background, as illustrated by EA
CNB	China Natural Background, as illustrated by GLOBE
CAB	China Anthropogenic Background, as illustrated by EA-GLOBE
GAB	Global Anthropogenic Background, as illustrated by BASE-GLOBE

4.3. Anthropogenic Versus Natural Contribution

China Natural Background (CNB, described in Table 2) is defined as surface O_3 concentrations over China in the absence of global anthropogenic emissions. CNB reveals the contribution of emissions from biomass burning, lightning, soil, and transport from the stratosphere. Figure 6 shows seasonal mean of CNB for 2000 and the ratio of CNB to BASE concentrations. CNB over EC varies by only about 5 ppbv between seasons, over a range from 15 to 30 ppbv with a gradient directed to the southeast. On the Tibetan Plateau, CNB is between 30 and 45 ppbv during spring and autumn, 40 and 55 in winter, and 25 and 35 during summer, accounting for more than 70% of the BASE O_3 concentrations in all but winter when the contribution is 50–60%. CNB over northwestern China is about 25–35 ppbv, accounting for about 70% of the surface O_3 there. Natural sources make important contributions to the surface O_3 over WC based on both the relatively large ratios and similar spatial patterns as BASE, while they are relatively less influential in EC.

Global Anthropogenic Background (GAB, described in Table 2) is defined as the difference between BASE (all emissions) and GLOBE (only natural emissions). GAB indicates the enhancement of surface O_3 above the natural background (GLOBE) due to global anthropogenic emissions. We also use the difference between EA and GLOBE to represent China Anthropogenic Background (CAB, described in Table 2), which indicates the enhancement of surface O_3 above the CNB (same as GLOBE, but simply over China)

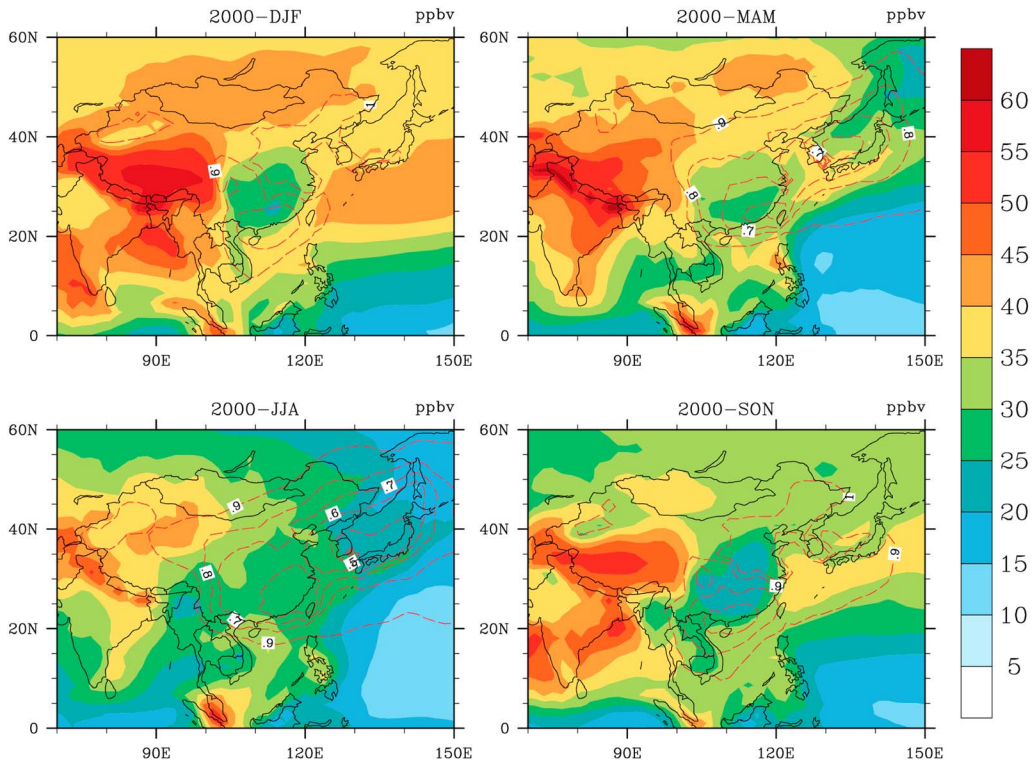

Figure 5. Spatial distributions of seasonal mean China Total Background (CTB) surface O_3 concentrations (ppbv) for DJF, MAM, JJA, and SON in 2000. These results are derived from the EA simulation (i.e., anthropogenic emissions from EA are turned off). Dashed lines stand for ratio of CTB to surface O_3 derived from BASE.

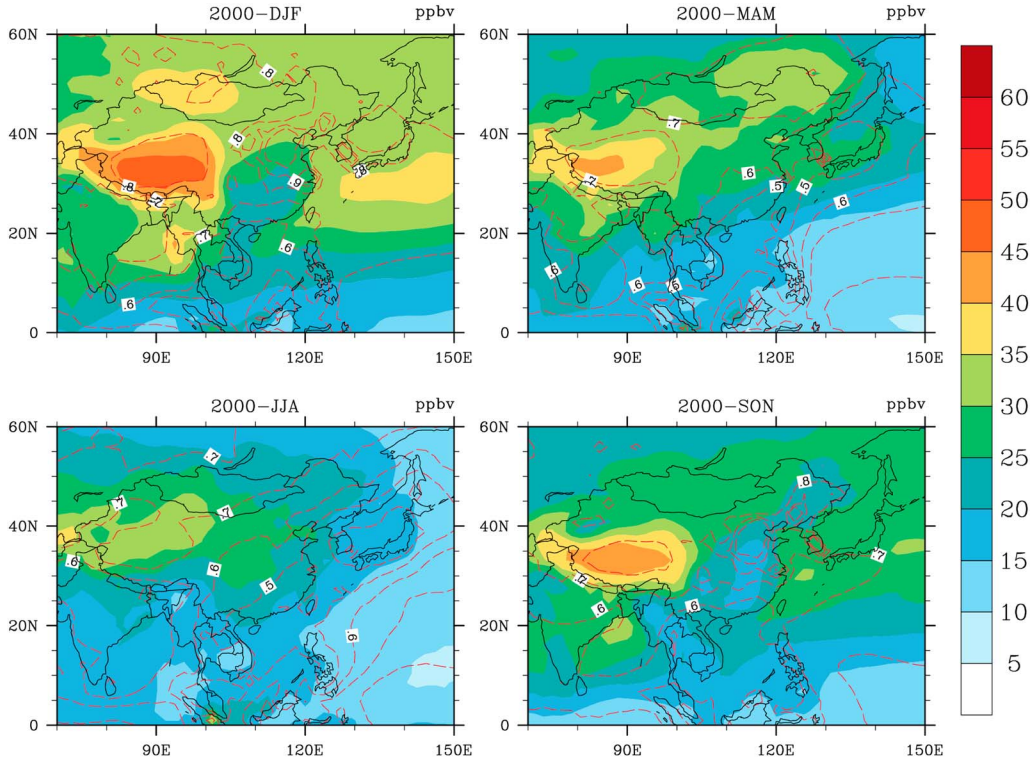

Figure 6. Spatial distributions of seasonal mean China Natural Background (CNB) surface ozone concentrations (ppbv) for DJF, MAM, JJA, and SON in 2000. These results are derived from the GLOBE simulation (all anthropogenic emissions of the world are turned off). Dashed lines stand for ratio of CNB to surface O_3 derived from BASE.

due to anthropogenic emissions from all regions outside China. GAB and CAB as defined here are different from the contribution from anthropogenic emissions, but to identify the influence from anthropogenic emissions on surface O_3 additional to natural emissions. The seasonal mean of CAB for 2000 and ratios of CAB to GAB are shown in Figure 7. CAB has greater impact in spring for 10–15 ppbv over WC and 5–10 ppbv over EC, whereas 0–5 ppbv over EC and 5–10 ppbv over WC during other seasons. This impact accounts for up to 90% in the Tibetan Plateau and 80% over Northwestern China of GAB during winter, spring, and autumn, decreasing to 60%–70% during summertime. However, over EC influence from CAB reduces to 20% of GAB during spring and summer, indicating a strong domestic emission impact. This indicates that surface O_3 over WC is significantly influenced by anthropogenic emissions originated outside of EA.

5. Influence From Individual Regions

Using an approach similar to that used to establish source-receptor relationships between U.S. states [*Tong and Mauzerall*, 2008], we establish source-receptor relationships between regions outside of China and surface ozone concentrations within China. In this analysis, we use the difference between BASE and each simulation including ME, IN, EU, MA, Southeast Asia (SEA), and SI to represent the influence of anthropogenic emissions from each region on global surface O_3 and on O_3 within China. The influence from an individual source region, as we define here, identifies the impact of removing emissions from that region and implies the benefit from air pollution mitigations in those regions. The difference of it from regional contributions, as well as the uncertainties associated with our analysis will be discussed in section 7.

Figure 8 shows the response of surface ozone to total anthropogenic emission reductions from each region during spring of 2000. Comparisons between influences from different regions indicate that Europe has the biggest impact on China's surface O_3 followed by India, the Middle East, Southeast Asia, Siberia, and mid-Asia. Emissions from Europe influence North China by more than 2 ppbv, central China by 1–2 ppbv, and South

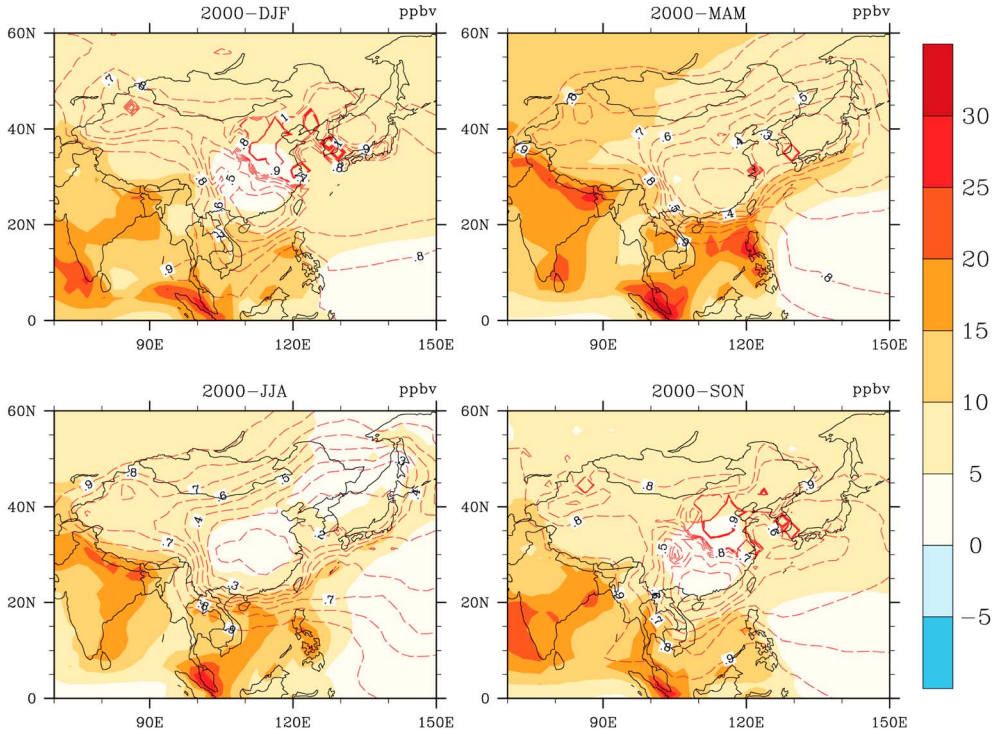

Figure 7. Spatial distributions of seasonal mean China Anthropogenic Background (CAB, derived by EA-GLOBE) surface ozone concentrations (ppbv) for DJF, MAM, JJA, and SON in 2000. Dashed lines stand for ratio of CAB to global anthropogenic background (GAB, derived by BASE-GLOBE).

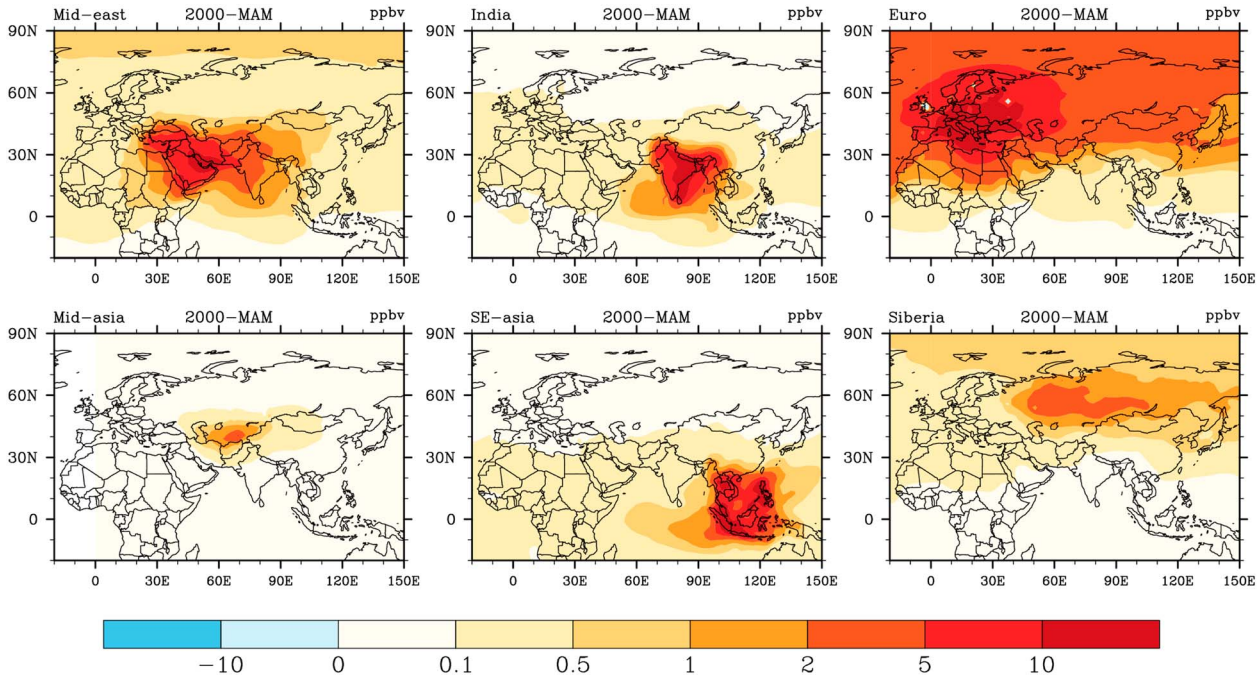

Figure 8. Effects of anthropogenic emissions from each region including ME, IN, EU, MA, SEA, and SI on the surface ozone concentrations (ppbv), during *MAM* of the model year 2000.

Table 3. Source-Receptor Relationship of Influence From Foreign Regions to Surface O_3 (ppbv) Over a Rectangular Region in Western China (30°N–45°N, 80°E–100°E)

	Middle East	India	Europe	Mid-Asia	SE Asia	Siberia
DJF	1.18	1.45	0.72	0.16	0.29	0.10
MAM	1.38	1.02	2.41	0.25	0.22	0.39
JJA	0.43	1.62	1.72	0.19	0.28	0.41
SON	1.15	0.89	0.83	0.18	0.28	0.16

China by 0.5–1 ppbv during springtime, while in summer influences from Europe are approximately 1 ppbv lower over all of China but are still more than 2 ppbv over Xinjiang. Indian emissions increase surface O_3 by up to 5 ppbv on the border and 1–5 ppbv on the Tibetan Plateau both in spring and summer. In summer, Southeast Asia extends its reach further north and enhances surface O_3 over Southern China by 0.5–1 ppbv, probably due to East Asia monsoon. Impacts from ME emissions show a gradient from 2 ppbv in WC to 0.5 ppbv in EC in spring, while falling to 0.1–0.5 ppbv in summer. Siberia has a relatively small impact on China's surface ozone of about 0.5–1 ppbv in northern most China and 0–0.5 in all other parts. Influence from mid-Asia is 0.5–1 ppbv in WC, and negligible in EC. Further analyses of year-round variations indicate proportional impact over China from the Middle East and India in winter and spring. This is possibly because winter features strong Westerlies at midlatitudes and strengthens the transport process despite low O_3 production during that period.

Located at midlatitudes, Western China is downwind to most Eurasian regions. Anthropogenic emissions from these regions enhance the surface O_3 over WC by 1–5 ppbv depending on location and season. Table 3 summarizes the influence from individual Eurasian regions to WC represented by a rectangular box (30°N–45°N, 80°E–100°E). The impact from EU (spring and autumn), IN (all year around), and ME (all seasons except summer) are particularly larger than other regions. Trans-Eurasian ozone transport thus appears to be an important component of hemispheric transport of air pollution.

6. Mechanism of Trans-Eurasian Transport

6.1. Seasonality of Trans-Eurasian Transport of Ozone

Influences from foreign sources to China's surface O_3 as described in section 5.2 are not necessarily due to transport of O_3 itself. O_3 precursors like NO_x (or its carrier peroxyacetylnitrate) can be transported to a receptor region and there react with locally emitted carbon monoxide or VOCs to produce O_3. Figure S1 in the supporting information shows the difference in the net chemical production rate of ozone between EA and GLOBE runs. This difference represents impacts from all foreign anthropogenic sources, including both production (positive) and destruction (negative). O_3 production rates resulting from foreign emissions are generally positive and higher in Northwest China than in EC, especially near the border. Horizontal O_3 flux, defined as mass of O_3 per unit volume transported through a vertical unit in a unit of time, is converted into ppbv d^{-1} km^{-2} in this study. It represents the intensity of horizontal transport. Figure 9 presents surface horizontal O_3 flux derived from CAB over Eurasia. In WC, horizontal flux is larger over the Tibetan Plateau than

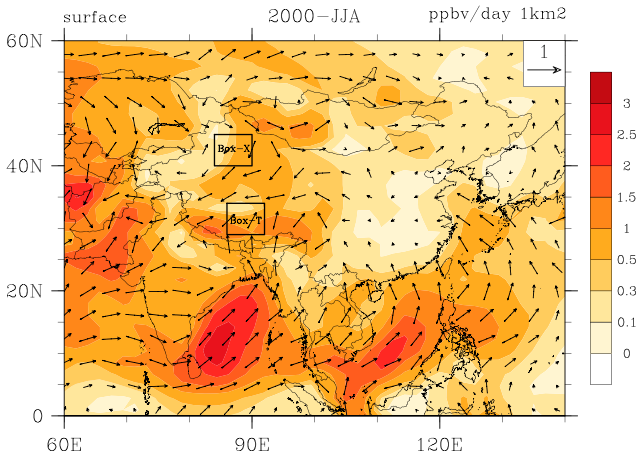

Figure 9. Difference in horizontal O_3 flux (ppbv d^{-1} km^{-2}) between EA and GLOBE on the surface level for the summer of 2000. Contours represent the intensity of the flux, and vectors stand for the direction. Receptor boxes over WC. Box-X (40°N–45°N, 84°E–90°E) is over Xinjiang, and Box-T (29°N–34°N, 86°E–92°E) is over Tibet. Arrows show transport paths of O_3 inflow.

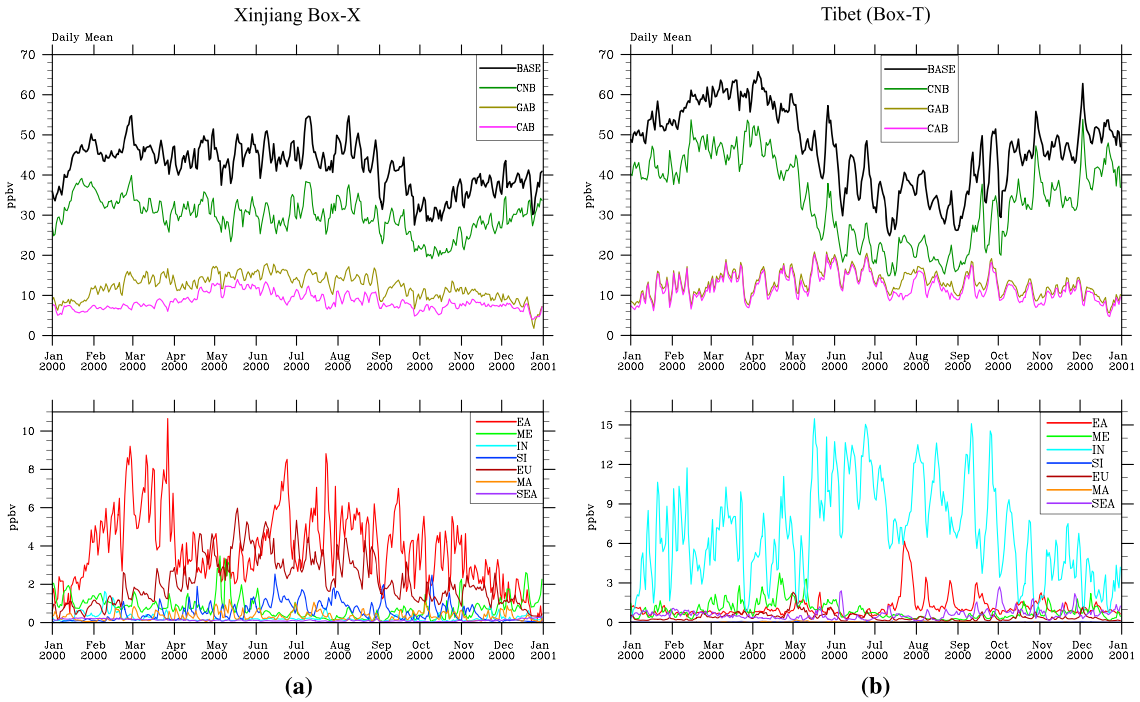

Figure 10. Time series of daily mean surface O_3 concentrations over (a) Xinjiang (Box-X) and (b) Tibet (Box-T) in 2000. (top row) Base is the effect from all emissions, CNB stands for the effect of natural emissions, GAB indicates the effect of global anthropogenic emissions, and CAB represents the effect of anthropogenic emissions from outside China. (bottom row) Each line stands for the effect of anthropogenic emissions from each region defined as in Table 1.

over Xinjiang, likely due to high surface O_3 concentrations over Tibet. Stronger mean inflow of O_3 occurs in WC from the Eurasian continent during spring and summer than in other seasons.

6.2. Episodic Influence due to Eurasian Emissions

In order to analyze the day-to-day variations of surface O_3 over WC, as well as influences from foreign sources, as shown in Figure 9 we use two receptor boxes: Box-X is over Xinjiang and Box-T is over the Tibetan Plateau. Figure 10 shows time series of daily mean O_3 concentrations at the surface over Box-X and Box-T in 2000. Over Xinjiang, EA anthropogenic emissions have the largest impact on surface O_3, followed by EU, SI, and the ME. Nonetheless, during spring and early summer, EU has a comparable influence to EA. Over Tibet, IN anthropogenic emissions dominate surface O_3 concentrations, while EA and the ME occasionally make substantial influences.

As described in section 6.2, we use peaks on BASE to represent episodic O_3 influences at the receptor region, and CAB and CNB for the anthropogenic and natural portion of these influences, respectively. For Box-X, episodic influences mainly arrive year round, whereas Box-T experiences a frequent impact from episodes except in winter. However, the anthropogenic influence to O_3 is strongest over Box-X in summer and spring while is pronounced year round over Box-T. Frequency of episodic influences is not fixed, but about once every 10–15 days during active seasons. Through comparisons between patterns of different lines, we can generally attribute these influences to their sources. Xinjiang (Box-X) is frequently influenced by episodic O_3 contributed by East Asia, Europe, and Siberia, and occasionally by the Middle East. The Tibetan Plateau is episodically influenced by emissions in India as well as natural sources (e.g., the large contribution from stratosphere-to-troposphere ozone exchange as indicated in *Zhao et al.* [2010]) year round, while occasionally by East Asia (probably due to the effect of summer monsoon) and Siberia, similar to the findings in *Zhao et al.* [2010]. The Middle East has frequent episodic O_3 influence on the Tibetan Plateau during spring and winter time.

Further analyses on spatial distributions of episodes find several main pathways as indicated by arrows on the border of WC in Figure 9. These pathways are active during spring and summer, bringing episodes of

12–15 ppbv anthropogenic portions to Box-X and 16–20 ppbv to Box-T. Long-range transport over midlatitude area from Europe to WC is mainly through episodic influence, with a high concentrations core of up to 20 ppbv anthropogenic portions. During spring and summer, when the weather pattern favors a tendency of lower pressure over Siberia and higher pressure over central Europe, the associated stronger westerlies tend to enhance the European influence over Box-X (see Figure S2 in the supporting information). However, for Box-T an above-normal high-pressure anomaly above Bangladesh tends to sweep more Indian pollutants to the Tibetan Plateau (Figure S3 in the supporting information).

7. Uncertainties in Ozone Contributions

In this study, we calculate the difference between full-emission and zero-emission simulations to represent the influence from individual regions, as well as combined sources (e.g., GAB and CAB), on China's surface O_3. This so-called perturbation method shows the impact of removing that source, which is different from real contributions from that source to current surface O_3 [*Grewe et al*., 2012]. The difference between the influence defined by our method and real contribution is much smaller over WC than over EC. As is shown in section 4.1, significantly low level of surface O_3 over EC during autumn and winter implies the occurrence of titration, and a NO_x-saturated regime at that time. However, WC, due to its relatively low NO_x emissions, is in NO_x-limited regime almost all year round [*Liu et al*., 2010]. Production of O_3 has a nonlinear relationship with its precursors, leading to a smaller value of the influence calculated by the perturbation method compared with the real contribution [*Emmons et al*., 2012]. This difference in NO_x-limited region is much weaker than in NO_x-saturated region created by perturbation method, because zeroing (i.e., 100% reducing) anthropogenic emissions would most probably switch NO_x-saturated region to NO_x-limited region [*Wu et al*., 2009], especially over heavily polluted EC. As our analyses mainly focus on WC, we believe that the influence calculated in this study is closer to real contribution compared with when the same method is used to study O_3 over EC.

Our zeroing-emission perturbation method implies how much surface O_3 over WC would be lowered if air pollution mitigation were implemented from individual regions over Eurasia. Although our method correctly indicates the amount of O_3 reduced over WC when the anthropogenic emissions from certain sources are entirely removed, uncertainties caused by the nonlinear relationship of O_3 production will still occur when using our results in certain ways for policy implications. The effect of mitigating 20% anthropogenic NO_x emissions from a source region on surface O_3 over WC, for example, will be underestimated if it is estimated by taking one fifth of our result from zeroing-emission method. This is because O_3 production efficiency increases with decreasing NO_x concentrations [*Sillman et al*., 1990], and zeroing-emissions from one region will enhance the efficiency of emissions from other regions. Furthermore, the complex coupling between different regions adds to the uncertainties in this study. The resulting uncertainties are nonnegligible when analyzing the influence from the source region on itself, EA in this case. However, as we mainly focus on influences from distant sources, the uncertainties over WC in this regard could be considered smaller than those over EC. The robustness of our results, particularly in terms of influences from individual regions, is also affected by the year of study (2000 in our case) for varying meteorological conditions and emissions, and the limited chemical substances/reactions included in MOZART-4. But the implications from our results are important qualitatively.

8. Conclusions

In this study, we use a global chemical transport model MOZART-4 to simulate source-receptor relationships of anthropogenic emissions from specific regions covering the Eurasian continent on surface O_3 concentrations over China. Model evaluation indicates that surface O_3 over inland areas are simulated well although coastal regions are generally overestimated and midlatitudes slightly underestimated. Surface O_3 concentrations over Western China are about 5–15 ppbv higher than over Eastern China, particularly during the winter half year. Over Western China, total background (as illustrated by China Total Background) accounts for approximately 90% of the surface O_3 concentrations, and natural background (as illustrated by China Natural Background) accounts for about 70%. However, over Eastern China, contributions from total background and natural background appear to be 60%–80% and 40%–60%, respectively, indicating a larger influence of domestic emissions. Further analyses of ratios of China Anthropogenic Background toward Global Anthropogenic

Background reveal that over Western China 60%–70% (summer) and more than 80% (other seasons) of the anthropogenic impact is attributed to foreign sources, whereas the ratio is much smaller over Eastern China. Foreign anthropogenic emissions mainly affect Western China, especially during springtime, while summertime foreign contributions to surface O_3 are small but nonnegligible because it accounts for the largest proportion of total concentrations (as illustrated by BASE).

We define influence from individual regions on surface O_3 over Western China as the difference between full-emission and zero-emission simulations using the perturbation method (or source-receptor relationship). Our definition is dedicated to implying benefits from air pollution mitigation from different regions. Nonlinear relationship of O_3 production with its precursors might affect further interpretation of our result for policy implications. The uncertainties associated with it are worth further investigation. Our results show that Europe has the biggest influence on China's surface ozone followed by India, the Middle East, Southeast Asia, Siberia, and middle Asia. These impacts are significant over Western China during spring and summer, while relatively small in winter and autumn, except those of the Middle East and India that have a similar magnitude throughout the year. We identify the importance of the transport of O_3 and its precursors from neighboring regions to Western China through the analysis of horizontal fluxes and chemical production rates that result from foreign sources. Time series of daily mean surface ozone over the Tibetan Plateau and Xinjiang reveal that East Asian anthropogenic emissions have the largest impact on surface O_3 (while the European is comparable during spring) over Xinjiang, and impact from Indian anthropogenic emissions dominates the anthropogenic surface O_3 over Tibet. Peaks on lines of O_3 time series indicate episodic influences on receptor regions. We can conclude from the occurrences of peaks that anthropogenic portion of episodic influences mainly takes effect in summer and spring over Xinjiang, while all year round over Tibetan Plateau, once every 10–15 days during their corresponding active seasons. These influences can all be attributed to emissions from East Asia, Europe, the Middle East, and Siberia over Xinjiang and to India and China over Tibet. We have also found main pathways through which episodic influences are transported toward Western China as indicated by Figure 9.

Previous studies regarding long-range transport of air pollutants have primarily focused on trans-Pacific and transatlantic transport. This study demonstrates that trans-Eurasian transport to Western China is also important. Furthermore, our study mainly focused on influences averaged over Western China, which may not well represent the actual impacts (e.g., over highly polluted areas that are strongly influenced by local emissions), in part due to missing information in the relatively coarse grid scales of the used model. Regarding the large population, high crop yields, and wide natural preservation area in Western China, more observations and model simulations of this region to further explore the mechanisms of O_3 transport and its potential impact would be valuable.

Acknowledgments

We thank two anonymous reviewers for their thoughtful comments and helpful suggestions. This work was supported by funding from the National Natural Science Foundation of China under awards 41222011, 41390240, and 41130754, the Research Project of Chinese Ministry of Education 113001A, the "863" Hi-Tech R&D Program of China under grant 2012AA063303, and the 111 Project (B14001).

References

Andreae, M. O., and P. Merlet (2001), Emission of trace gases and aerosols from biomass burning, *Global Biogeochem. Cycles*, *15*(4), 955–966.

Avnery, S., D. L. Mauzerall, J. F. Liu, and L. W. Horowitz (2011), Global crop yield reductions due to surface ozone exposure: 1. Year 2000 crop production losses and economic damage, *Atmos. Environ.*, *45*(13), 2284–2296.

Baughcum, S., T. Tritz, S. Henderson, and D. Pickett (1996), Scheduled civil aircraft emission inventories for 1992: Database development and analysis, *NASA Contractor Rep. 4700*, 196 pp., NASA, Langley Res. Cent., Hampton, Va.

Baughcum, S. L., D. J. Sutkus Jr., and S. C. Hendersonm (1998), Year 2015 aircraft emission scenario for scheduled air traffic, *NASA-CR-1998-207638*, 44 pp., NASA, Langley Res. Cent., Hampton, Va.

Bond, T. C., D. G. Streets, K. F. Yarber, S. M. Nelson, J. H. Woo, and Z. Klimont (2004), A technology-based global inventory of black and organic carbon emissions from combustion, *J. Geophys. Res.*, *109*, D14203, doi:10.1029/2003JD003697.

Brown-Steiner, B., and P. Hess (2011), Asian influence on surface ozone in the United States: A comparison of chemistry, seasonality, and transport mechanisms, *J. Geophys. Res.*, *116*, D17309, doi:10.1029/2011JD015846.

China Statistical Yearbook (2013), *National Bureau of Statistic of China*, China Statistic Press, Beijing.

David, L. M., and P. R. Nair (2011), Diurnal and seasonal variability of surface ozone and NOx at a tropical coastal site: Association with mesoscale and synoptic meteorological conditions, *J. Geophys. Res.*, *116*, D10303, doi:10.1029/2010JD015076.

Ding, A. J., and T. Wang (2006), Influence of stratosphere-to-troposphere exchange on the seasonal cycle of surface ozone at Mount Waliguan in Western China, *Geophys. Res. Lett.*, *33*, L03803, doi:10.1029/2005GL024760.

Emmons, L. K., et al. (2010), Description and evaluation of the model for ozone and related chemical tracers, version 4 (MOZART-4), *Geosci. Model Dev.*, *3*, 43–67.

Emmons, L. K., P. G. Hess, J. F. Lamarque, and G. G. Pfister (2012), Tagged ozone mechanism for MOZART-4, CAM-chem and other chemical transport models, *Geosci. Model Dev.*, *5*(6), 1531–1542.

Fishman, J. (1991), Comment on Tropical cyclone-upper-atmospheric interaction as inferred from satellite total ozone observations, *J. Appl. Meteorol.*, *30*(7), 1047–1048.

Granier, C., et al. (2005), POET, a database of surface emissions of ozone precursors. [Available at http://www.aero.jussieu.fr/projet/ACCENT/POET.php.]

Grewe, V., K. Dahlmann, S. Matthes, and W. Steinbrecht (2012), Attributing ozone to NOx emissions: Implications for climate mitigation measures, *Atmos. Environ.*, *59*, 102–107.

Gryparis, A., et al. (2004), Acute effects of ozone on mortality from the "Air pollution and health: A European approach" project, *Am. J. Respir. Crit. Care Med.*, *170*(10), 1080–1087.

Guenther, A., T. Karl, P. Harley, C. Wiedinmyer, P. I. Palmer, and C. Geron (2006), Estimates of global terrestrial isoprene emissions using MEGAN (Model of Emissions of Gases and Aerosols from Nature), *Atmos. Chem. Phys.*, *6*, 3181–3210.

Hemispheric Transport of Air Pollution (2010), Task Force on Hemispheric Transport of Air Pollution (TF HTAP), Hemispheric Transport of Air Pollution. United Nations Economic Commission for Europe: Geneva (GE.11-22134–June 201 1–2,130) Rep.

Honrath, R. E., R. C. Owen, M. Val Martin, J. S. Reid, K. Lapina, P. Fialho, M. P. Dziobak, J. Kleissl, and D. L. Westphal (2004), Regional and hemispheric impacts of anthropogenic and biomass burning emissions on summertime CO and O_3 in the North Atlantic lower free troposphere, *J. Geophys. Res.*, *109*, D24310, doi:10.1029/2004JD005147.

Hsu, J., M. J. Prather, and O. Wild (2005), Diagnosing the stratosphere-to-troposphere flux of ozone in a chemistry transport model, *J. Geophys. Res.*, *110*, D19305, doi:10.1029/2005JD006045.

Huntrieser, H., et al. (2005), Intercontinental air pollution transport from North America to Europe: Experimental evidence from airborne measurements and surface observations, *J. Geophys. Res.*, *110*, D01305, doi:10.1029/2004JD005045.

Jacob, D. J., J. A. Logan, and P. P. Murti (1999), Effect of rising Asian emissions on surface ozone in the United States, *Geophys. Res. Lett.*, *26*(14), 2175–2178, doi:10.1029/1999GL900450.

Jain, S. L., B. C. Arya, A. Kumar, S. D. Ghude, and P. S. Kulkarni (2005), Observational study of surface ozone at New Delhi, India, *Int. J. Remote Sens.*, *26*(16), 3515–3524.

Li, J., Z. F. Wang, H. Akimoto, C. Gao, P. Pochanart, and X. Q. Wang (2007), Modeling study of ozone seasonal cycle in lower troposphere over East Asia, *J. Geophys. Res.*, *112*, D22S25, doi:10.1029/2006JD008209.

Li, Q. B., et al. (2001), A tropospheric ozone maximum over the Middle East, *Geophys. Res. Lett.*, *28*(17), 3235–3238, doi:10.1029/2001GL013134.

Lin, M. Y., et al. (2012), Transport of Asian ozone pollution into surface air over the western United States in spring, *J. Geophys. Res.*, *117*, D00V07, doi:10.1029/2011JD016961.

Liu, J., D. L. Mauzerall, and L. W. Horowitz (2005), Analysis of seasonal and interannual variability in transpacific transport, *J. Geophys. Res.*, *110*, D04302, doi:10.1029/2004JD005207.

Liu, J. F., and D. L. Mauzerall (2005), Estimating the average time for inter-continental transport of air pollutants, *Geophys. Res. Lett.*, *32*, L11814, doi:10.1029/2005GL022619.

Liu, J. J., D. B. A. Jones, J. R. Worden, D. Noone, M. Parrington, and J. Kar (2009), Analysis of the summertime buildup of tropospheric ozone abundances over the Middle East and North Africa as observed by the Tropospheric Emission Spectrometer instrument, *J. Geophys. Res.*, *114*, D07399, doi:10.1029/2009JD012045.

Liu, J. J., D. B. A. Jones, S. L. Zhang, and J. Kar (2011), Influence of interannual variations in transport on summertime abundances of ozone over the Middle East, *J. Geophys. Res.*, *116*, D20310, doi:10.1029/2011JD016188.

Liu, X.-H., Y. Zhang, J. Xing, Q. Zhang, K. Wang, D. G. Streets, C. Jang, W.-X. Wang, and J.-M. Hao (2010), Understanding of regional air pollution over China using CMAQ, Part II. Process analysis and sensitivity of ozone and particulate matter to precursor emissions, *Atmos. Environ.*, *44*, 3719–3727.

Ma, J., X. Zheng, and X. Xu (2005), Comment on "Why does surface ozone peak in summertime at Waliguan?" by Bin Zhu et al., *Geophys. Res. Lett.*, *32*, L01805, doi:10.1029/2004GL021683.

Marrero, W., S. W. North, and J. Geidosch (2011), Diurnal variation of NOx and ozone in urban and rural areas in southeastern Texas, Abstr Pap Am Chem S, 241.

Martin, M. V., R. E. Honrath, R. C. Owen, G. Pfister, P. Fialho, and F. Barata (2006), Significant enhancements of nitrogen oxides, black carbon, and ozone in the North Atlantic lower free troposphere resulting from North American boreal wildfires, *J. Geophys. Res.*, *111*, D23s60, doi:10.1029/2006JD007530.

Martin, R. V. (2008), Satellite remote sensing of surface air quality, *Atmos. Environ.*, *42*(34), 7823–7843.

Mauzerall, D. L., and X. P. Wang (2001), Protecting agricultural crops from the effects of tropospheric ozone exposure: Reconciling science and standard setting in the United States, Europe, and Asia, *Annu. Rev. Energy Environ.*, *26*, 237–268.

McLinden, C. A., S. C. Olsen, B. Hannegan, O. Wild, M. J. Prather, and J. Sundet (2000), Stratospheric ozone in 3-D models: A simple chemistry and the cross-tropopause flux, *J. Geophys. Res.*, *105*(D11), 14,653–14,665, doi:10.1029/2000JD900124.

Mortlock, A., and R. V. Alstyne (1998), Military, charter, unreported domestic traffic and general aviation: 1976, 1984, 1992, and 2015 emission scenarios, *NASA CR-1998-207639*, 118 pp., NASA, Langley Res. Cent., Hampton, Va.

Naja, M., and S. Lal (2002), Surface ozone and precursor gases at Gadanki (13.5°N, 79.2°E), a tropical rural site in India, *J. Geophys. Res.*, *107*(D14), 4197, doi:10.1029/2001JD000357.

Naja, M., S. Lal, and D. Chand (2003), Diurnal and seasonal variabilities in surface ozone at a high altitude site Mt Abu (24.6°N, 72.7°E, 1680 m asl) in India, *Atmos. Environ.*, *37*(30), 4205–4215.

Ohara, T., H. Akimoto, J. Kurokawa, N. Horii, K. Yamaji, X. Yan, and T. Hayasaka (2007), An Asian emission inventory of anthropogenic emission sources for the period 1980–2020, *Atmos. Chem. Phys.*, *7*(16), 4419–4444.

Olivier, J., and J. Berdowski (2001), *The Climate System, Chap. Global Emissions Sources and Sinks*, A.A. Balkema Publishers/Swets, Zeitlinger Publishers, Lisse, Netherlands.

Olivier, J., J. Peters, C. Granier, G. Petron, J. Muller, and S. Wallens (2003), Present and future surface emissions of atmospheric compounds, POET Rep. 2, EU project EVK2-1999-00011.

Owen, R. C., O. R. Cooper, A. Stohl, and R. E. Honrath (2006), An analysis of the mechanisms of North American pollutant transport to the central North Atlantic lower free troposphere, *J. Geophys. Res.*, *111*, D23S58, doi:10.1029/2006JD007062.

Pochanart, P., J. Hirokawa, Y. Kajii, H. Akimoto, and M. Nakao (1999), Influence of regional-scale anthropogenic activity in northeast Asia on seasonal variations of surface ozone and carbon monoxide observed at Oki, Japan, *J. Geophys. Res.*, *104*(D3), 3621–3631, doi:10.1029/1998JD100071.

Pochanart, P., J. Kreasuwun, P. Sukasem, W. Geeratithadaniyom, M. S. Tabucanon, J. Hirokawa, Y. Kajii, and H. Akimoto (2001), Tropical tropospheric ozone observed in Thailand, *Atmos. Environ.*, *35*(15), 2657–2668.

Pochanart, P., H. Akimoto, Y. Kajii, V. M. Potemkin, and T. V. Khodzher (2003), Regional background ozone and carbon monoxide variations in remote Siberia/East Asia, *J. Geophys. Res.*, *108*(D1), 4028, doi:10.1029/2001JD001412.

Ran, L., W. L. Lin, Y. Z. Deji, B. La, P. M. Tsering, X. B. Xu, and W. Wang (2014), Surface gas pollutants in Lhasa, a highland city of Tibet: Current levels and pollution implications, *Atmos. Chem. Phys. Discuss.*, *14*, 11,787–11,814.

Rodgers, E., J. Stout, J. Steranka, and S. Chang (1991), Comment on Tropical cyclone-upper-atmospheric interaction as inferred from satellite total ozone observations—Reply, *J. Appl. Meteorol.*, *30*(7), 1049–1049.

Shindell, D., et al. (2012), Simultaneously mitigating near-term climate change and improving human health and food security, *Science*, *335*(6065), 183–189.
Sillman, S., J. A. Logan, and S. C. Wofsy (1990), The sensitivity of ozone to nitrogen oxides and hydrocarbons in regional ozone episodes, *J. Geophys. Res.*, *95*(D2), 1837–1851, doi:10.1029/JD095iD02p01837.
Stohl, A., C. Forster, S. Eckhardt, N. Spichtinger, H. Huntrieser, J. Heland, H. Schlager, S. Wilhelm, F. Arnold, and O. Cooper (2003), A backward modeling study of intercontinental pollution transport using aircraft measurements, *J. Geophys. Res.*, *108*(D12), 4370, doi:10.1029/2002JD002862.
Sutkus, D. J., Jr., S. L. Baughcum, and D. P. DuBois (2001), Scheduled civil aircract emission inventories for 1999: Database development and analysis, *NASA-CR-2001-211216*.
Tang, G., Y. Wang, X. Li, D. Ji, S. Hsu, and X. Gao (2012), Spatial-temporal variations in surface ozone in Northern China as observed during 2009–2010 and possible implications for future air quality control strategies, *Atmos. Chem. Phys.*, *12*, 2757–2776.
Tie, X. X., S. Madronich, S. Walters, R. Y. Zhang, P. Rasch, and W. Collins (2003), Effect of clouds on photolysis and oxidants in the troposphere, *J. Geophys. Res.*, *108*(D20), 4642, doi:10.1029/2003JD003659.
Tong, D. Q., and D. L. Mauzerall (2008), Summertime state-level source-receptor relationships between nitrogen oxides emissions and surface ozone concentrations over the continental United States, *Environ. Sci. Technol.*, *42*(21), 7976–7984.
Trickl, T., O. R. Cooper, H. Eisele, P. James, R. Mucke, and A. Stohl (2003), Intercontinental transport and its influence on the ozone concentrations over central Europe: Three case studies, *J. Geophys. Res.*, *108*(D12), 8530, doi:10.1029/2002JD002735.
van der Werf, G. R., J. T. Randerson, L. Giglio, G. J. Collatz, P. S. Kasibhatla, and A. F. Arellano (2006), Interannual variability in global biomass burning emissions from 1997 to 2004, *Atmos. Chem. Phys.*, *6*, 3423–3441.
Wang, T., V. T. F. Cheung, M. Anson, and Y. S. Li (2001), Ozone and related gaseous pollutants in the boundary layer of Eastern China: Overview of the recent measurements at a rural site, *Geophys. Res. Lett.*, *28*(12), 2373–2376, doi:10.1029/2000GL012378.
Wang, T., X. L. Wei, A. J. Ding, C. N. Poon, K. S. Lam, Y. S. Li, L. Y. Chan, and M. Anson (2009), Increasing surface ozone concentrations in the background atmosphere of Southern China, 1994–2007, *Atmos. Chem. Phys.*, *9*(16), 6216–6226.
Wang, X. P., and D. L. Mauzerall (2004), Characterizing distributions of surface ozone and its impact on grain production in China, Japan and South Korea: 1990 and 2020, *Atmos. Environ.*, *38*(26), 4383–4402.
Wang, Y., M. B. McElroy, J. W. Munger, J. Hao, H. Ma, C. P. Nielsen, and Y. Chen (2008), Variations of O-3 and CO in summertime at a rural site near Beijing, *Atmos. Chem. Phys.*, *8*(21), 6355–6363.
Wang, Y., Y. Zhang, J. Hao, and M. Luo (2011), Seasonal and spatial variability of surface ozone over China: Contributions from background and domestic pollution, *Atmos. Chem. Phys.*, *11*, 3511–3525.
Wang, Y., L. Shen, S. Wu, L. Mickley, J. He, and J. Hao (2013), Sensitivity of surface ozone over China to 2000–2050 global changes of climate and emissions, *Atmos. Environ.*, *75*, 374–382.
West, J. J., A. M. Fiore, L. W. Horowitz, and D. L. Mauzerall (2006), Global health benefits of mitigating ozone pollution with methane emission controls, *Proc. Natl. Acad. Sci. U.S.A.*, *103*(11), 3988–3993.
West, J. J., V. Naik, L. W. Horowitz, and A. M. Fiore (2009), Effect of regional precursor emission controls on long-range ozone transport—Part 2: Steady-state changes in ozone air quality and impacts on human mortality, *Atmos. Chem. Phys.*, *9*(16), 6095–6107.
Wild, O., P. Pochanart, and H. Akimoto (2004), Trans-Eurasian transport of ozone and its precursors, *J. Geophys. Res.*, *109*, D11302, doi:10.1029/2003JD004501.
World Health Organization (2006), Global update 2005: Particulate matter, ozone, nitrogen dioxide, and sulfur dioxide, edited, World Health Organ., Geneva, Switzerland. [Available at http://whqlibdoc.who.int/hq/2006/WHO_SDE_PHE_OEH_06.02_eng.pdf.]
Wu, S., B. N. Duncan, D. J. Jacob, A. M. Fiore, and O. Wild (2009), Chemical nonlinearities in relating intercontinental ozone pollution to anthropogenic emissions, *Geophys. Res. Lett.*, *36*, L05806, doi:10.1029/2008GL036607.
Xue, L. K., et al. (2011), Source of surface ozone and reactive nitrogen speciation at Mount Waliguan in western China: New insights from the 2006 summer study, *J. Geophys. Res.*, *116*, D07306, doi:10.1029/2010JD014735.
Yang, Q., Y. H. Wang, C. Zhao, Z. Liu, W. I. Gustafson, and M. Shao (2011), NOx emission reduction and its effects on ozone during the 2008 Olympic Games, *Environ. Sci. Technol.*, *45*(15), 6404–6410.
Yang, W.-Y., J. Li, H.-S. Chen, Z.-F. Wang, B. Hu, T. Song, and J.-J. Li (2014), Modeling analysis of boundary layer ozone distributions over East Asia, *China Environ. Sci.*, *34*(7), 1633–1641.
Zhao, C., Y. Wang, and T. Zeng (2009), East China plains: A "Basin" of ozone pollution, *Environ. Sci. Technol.*, *43*, 1911–1915.
Zhao, C., Y. Wang, Q. Yang, R. Fu, D. Cunnold, and Y. Choi (2010), Impact of East Asian summer monsoon on the air quality over China: View from space, *J. Geophys. Res.*, *115*, D09301, doi:10.1029/2009JD012745.
Zhu, B., H. Akimoto, Z. Wang, K. Sudo, J. Tang, and U. Itsushi (2004), Why does surface ozone peak in summertime at Waliguan?, *Geophys. Res. Lett.*, *31*, L17104, doi:10.1029/2004GL020609.